

# CONFINEMENT EFFICACY OF PARTIALLY AND FULLY WRAPPED CFRP SYSTEMS IN RC COLUMN PROTOTYPES

**Ferreira, D.R.S.M.**

*Pf.D. Candidate, Dep. of Civil Engeneering, University of Minho, Campus de Azurém 4800-058 Guimarães, Portugal*

**Barros, J.A.O.**

*Associate Prof., Dep. of Civil Engeneering, University of Minho, Campus de Azurém 4800-058 Guimarães, Portugal*

## INTRODUCTION

Since the beginning of the nineties, fibre reinforced polymers (FRP) have been used to increase the load carrying capacity and the energy absorption capacity of reinforced concrete columns [1-5]. The high specific strength and stiffness, the low thickness and weight, and the high resistance to corrosion of FRP materials are favourable properties justifying the increase use of these composites in the structural upgrading [6]. The full wrapping FRP-technique is the most used to increase the load carrying capacity and the energy absorption capacity of reinforced concrete (RC) columns. However, preliminary tests with concrete elements submitted to direct compressive loading revealed that partial wrapping (strips of CFRP sheets) is a promising confinement technique [7]. Since in concrete columns deserving strengthening intervention there are always a certain percentage of steel hoops, the application of CFRP strips in-between the existent steel hoops can be an adjusted confinement technique with technical and economical advantages, when full wrapping is taken for basis of comparison. To assess the efficacy of the partial wrapping technique, 108 prototypes of RC columns were confined by distinct CFRP arrangements and tested under direct compression. The experimental program was designed to evaluate the influence of the following variables on the compression behavior: stiffness of the wet lay-up CFRP sheet; distance between CFRP strips; width of the CFRP strip; number of CFRP layers per each strip; concrete strength; percentage of the steel longitudinal and transversal reinforcement ratios. The present work describes the experimental program and presents and analyzes the obtained results. Using the obtained experimental results, the applicability of a confinement model [8] was appraised for the RC columns partially wrapped.

**Keywords:** concrete, CFRP, confinement

## CONFINEMENT ARRANGEMENTS AND EXPERIMENTAL PROGRAM

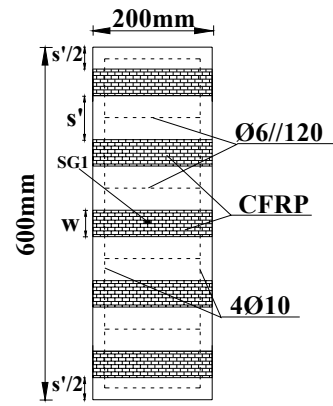
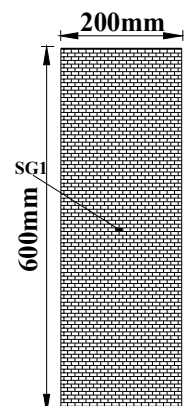
The experimental program deals with direct compression tests with RC column elements of 600 mm length and 200 mm diameter. This program is composed by several groups of tests in order to evaluate the influence of the following parameters on the compressive strength and deformation capacity of RC elements submitted, predominantly, to compressive loading: concrete strength class (two average compressive strengths, 15 MPa and 32 MPa); stiffness of the confinement CFRP system (two CFRP sheets, one of 300 g/m<sup>2</sup> of fibers and the other of 200 g/m<sup>2</sup> of fibers); width (W) and spacing (s') of the CFRP strips; number of CFRP layers per strip (L); percentage of the longitudinal and transversal steel reinforcement ( $\rho_{sl}$ ,  $\rho_{st}$ ), see Tab. 1. Due to lack of space, only the groups of tests C15S200 $\phi$ 10, C15S300 $\phi$ 10, C32S200 $\phi$ 8 and C32S300 $\phi$ 8, indicated in Tab. 1, are analyzed in the present paper. In this designation, Cxx means specimens of a concrete of average compressive strength of xx MPa, while S200 and S300 indicate the type

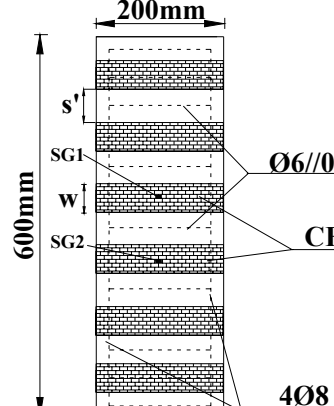
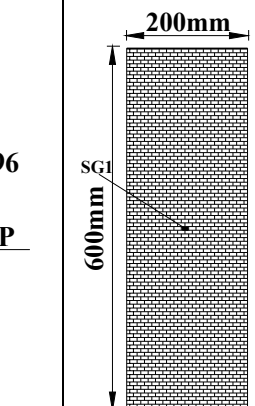
of CFRP sheet, 200 g/m<sup>2</sup> and 300 g/m<sup>2</sup>, respectively. Finally,  $\phi_j$  indicates the diameter, in mm, of the steel longitudinal bars.

Two groups were confined with a CFRP sheet of 300 g/m<sup>2</sup> of fibers (C15S300 $\phi$ 10, C32S300 $\phi$ 8), while the specimens of the other two groups (C15S200 $\phi$ 10, C32S200 $\phi$ 8) were confined with a CFRP sheet of 200 g/m<sup>2</sup> of fibers.

The average concrete compressive strength ( $f_{cm}$ ) of the groups C15S200 $\phi$ 10 and C15S300 $\phi$ 10 was 15 MPa, while the  $f_{cm}$  of groups C32S200 $\phi$ 8 and C32S300 $\phi$ 8 was 32 MPa. The two former groups were reinforced longitudinally with four steel bars of 10 mm diameter, whereas four steel bars of 8 mm diameter were applied in the last two groups. Following the recommendations of the Portuguese Code for RC structures, the spacing of the steel hoops was considered 12 times the diameter of the longitudinal bars. In the discrete confinement arrangements the strips were placed at mid distance between two consecutive steel hoops. Each group of tests is constituted by three series that are distinguished by the width of the CFRP strip: 45 mm (W45), 60 mm (W60) and 600 mm (W600 – fully-wrapped). As Fig. 1 shows, the partially-wrapped specimens of C15S200 $\phi$ 10 and C15S300 $\phi$ 10 groups are confined by five strips (W45S5 and W60S5), while the partially-wrapped specimens of C32S200 $\phi$ 8 and C32S300 $\phi$ 8 groups are confined by six strips (W45S6 and W60S6). Each one of these test series is composed by two sub-series, one of three layers per strip (L3) and the other with five layers per strip (L5). Previous research revealed that, above five layers per strip, the benefits in terms of specimen load carrying capacity and energy absorption capacity are marginal [9].

**Tab. 1.** Experimental program.

					
W [mm]	Designation	s' [mm]	W [mm]	Designation	
45	W45S5L3	75	600	W600S1L3	
	W45S5L5			W600S1L5	
60	W60S5L3	60			
	W60S5L5				
Concrete average compressive strength: 15 MPa					
Longitudinal bars: $\phi$ 10					
Type of CFRP sheet	CF120 S&P 240 (200 gm/m <sup>2</sup> )	Group of test series	C15S200 $\phi$ 10		
	CF130 S&P 240 (300 gm/m <sup>2</sup> )		C15S300 $\phi$ 10		

					
W [mm]	Designation	s' [mm]	W [mm]	Designation	
45	W45S6L3	55	600	W600S1L3	
	W45S6L5			W600S1L5	
60	W60S6L3	40			
	W60S6L5				
Concrete average compressive strength: 32 MPa					
Longitudinal bars: $\phi$ 8					
Type of CFRP sheet	CF120 S&P 240 (200 gm/m <sup>2</sup> )	Group of test series	C32S200 $\phi$ 8		
	CF130 S&P 240 (300 gm/m <sup>2</sup> )		C32S300 $\phi$ 8		

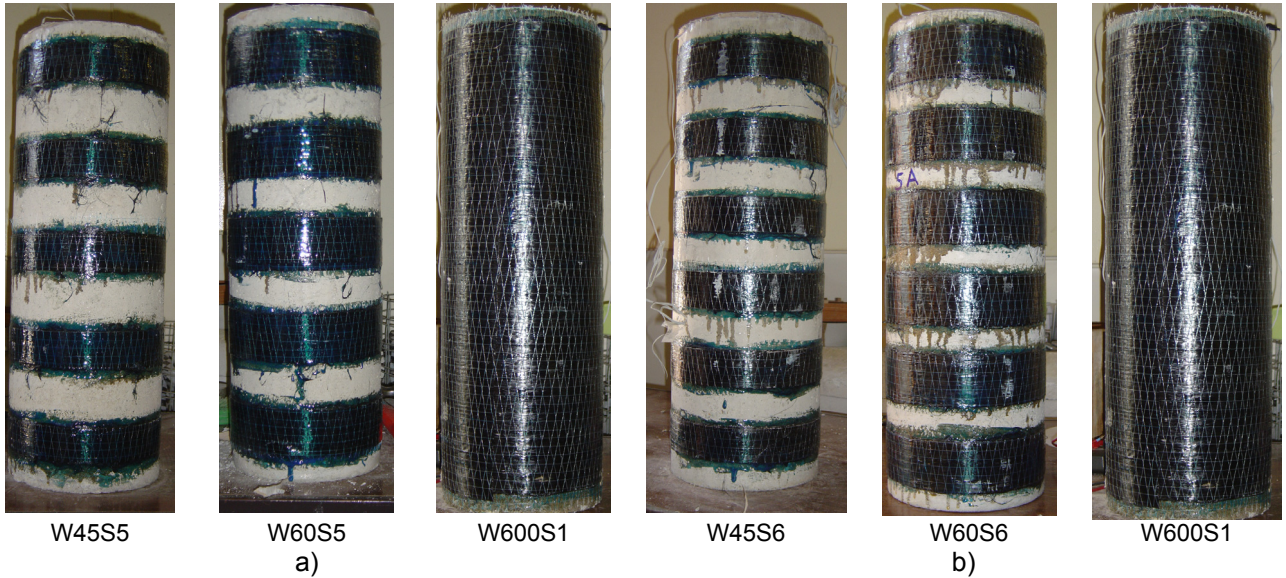


**Fig. 1.** Confinement systems: a) C15S200 $\phi$ 10 and C15S300 $\phi$ 10 groups; b) C32S200 $\phi$ 8 and C32S300 $\phi$ 8.

## MATERIALS

From direct compression tests carried out at 28 days with three concrete cylinder specimens of 150 mm diameter and 300 mm height, average compressive strength of 15 MPa and 32 MPa was obtained for the concrete of the groups C15S200 $\phi$ 10, C15S300 $\phi$ 10, and C32S200 $\phi$ 10, C32S300 $\phi$ 10, respectively.

The CFRP sheets used have the trade name of CF 120 S&P 240 (200 g/m<sup>2</sup> of fibers) and CF 130 S&P 240 (300 g/m<sup>2</sup> of fibers). According to the supplier, CF 120 and CF 130 sheets have a thickness of 0.117 mm and 0.176 mm, respectively, and have a tensile strength higher than 3700 MPa, and an elasticity modulus and an ultimate strain in the fibre direction of about 240 GPa and 15%, respectively. To check the values of these properties, samples of CFRP were tested according to ISO recommendations [10]. The tensile specimen configuration is represented in Fig. 2. To avoid localized fracture at the specimen's extremities fixed to the machine grips, layers of the same CFRP sheet were epoxy-glued to these extremities, as represented in Fig. 2. The strains were measured from a clip gauge of 50 mm of measuring length and 0.5% accuracy, see Fig. 3. The tests were carried out under displacement control at a rate of 1 mm/minute. The obtained results are presented in Tab. 2. The values determined experimentally for the thickness, included in Tab. 2, were used in the evaluation of the elasticity modulus and tensile strength of the CFRP sheets.

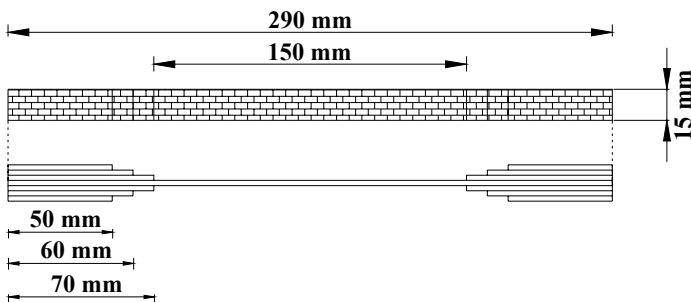


**Fig. 2.** CFRP tensile test specimen.

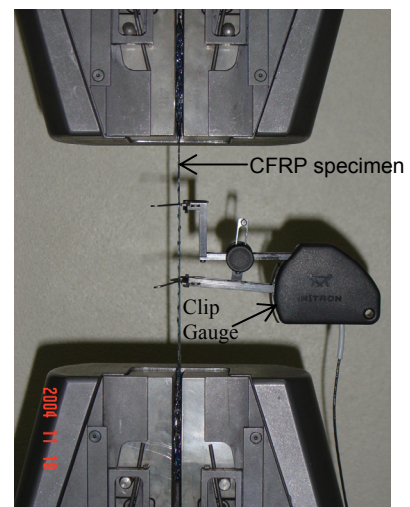


**Fig. 3.** CFRP specimen being tested in direct tension.

**Tab. 2.** CFRP properties (average of five tests).

CFRP Sheets	Thickness (mm)	Tensile strength (MPa)	Ultimate strain (%)	Elasticity modulus (GPa)
CF120	0.113	3535	1.52	232
CF130	0.176	3070	1.33	230

## TEST SETUP

Three displacement transducers were positioned at 120 degrees around the specimen and registered the displacements between the steel load plates of the equipment (see Fig. 4). This test setup avoids that the deformation of the test equipment is added to the values recorded by the LVDTs. Taking the values registered in these displacement transducers, the displacement at the specimen axis was determined for each scan reading [9], and the corresponding strain was obtained dividing this displacement by the measured specimen's initial height. To decrease the restriction imposed by the machine load plates to the radial expansion of the specimen's extremities, a system of two sheets of Teflon with oil between them was applied in-between the bottom plate of the machine and the bottom specimen's extremity. The Teflon system was not applied in-between the top plate and the top specimen's extremity, since this plate was connected to a spherical steel hinge. Strains in the CFRP fiber direction were measured by strain gauges (SG1 and SG2) fixed on the specimen according to the arrangements indicated in the sketches into Tab. 1. A detailed description of the test equipment and test procedures can be found elsewhere [9].

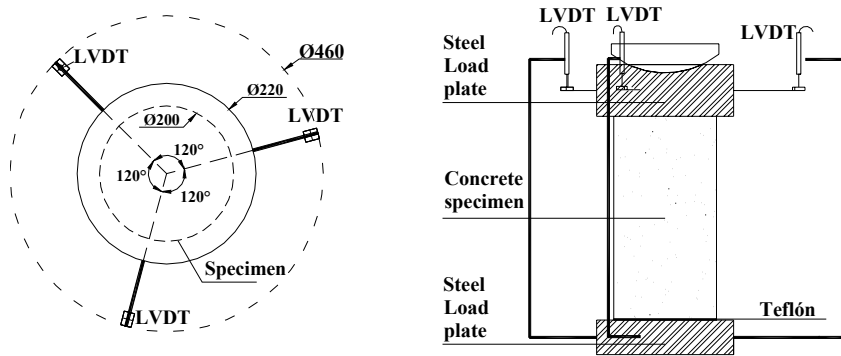


**Fig. 4.** Position of the LVDTs.

## EXPERIMENTAL RESULTS

### Groups C15S200φ10 and C15S300φ10

Figs. 5 and 6 show the relationships between concrete stress and both the concrete axial strain and the CFRP strain in the fiber direction for the series of the groups of tests C15S200φ10 and C15S300φ10. Each curve represents the average response registered in the two specimens that compose each series. The concrete stress is the ratio between the applied load and the specimen cross section. In these figures, UPC represents the unconfined plain concrete specimens, URC,φ10 the unconfined reinforced (longitudinally and transversally) concrete specimens. In each graph, the CFRP confinement ratio,  $\rho_f = A_f/A_{c,t}$ , is also included, where  $A_f = 2 \times S \times W \times L \times t_f \text{ mm}^2$  is the cross sectional area of the confinement system ( $t_f$  is the thickness of the CFRP sheet), and  $A_{c,t}$  is the area of specimen longitudinal cross section ( $A_{c,t} = 200 \times 600 \text{ mm}^2$ ). In general, the stress-strain relationship of the confined specimens is composed by two quasi-linear branches, connected by a nonlinear transition branch.

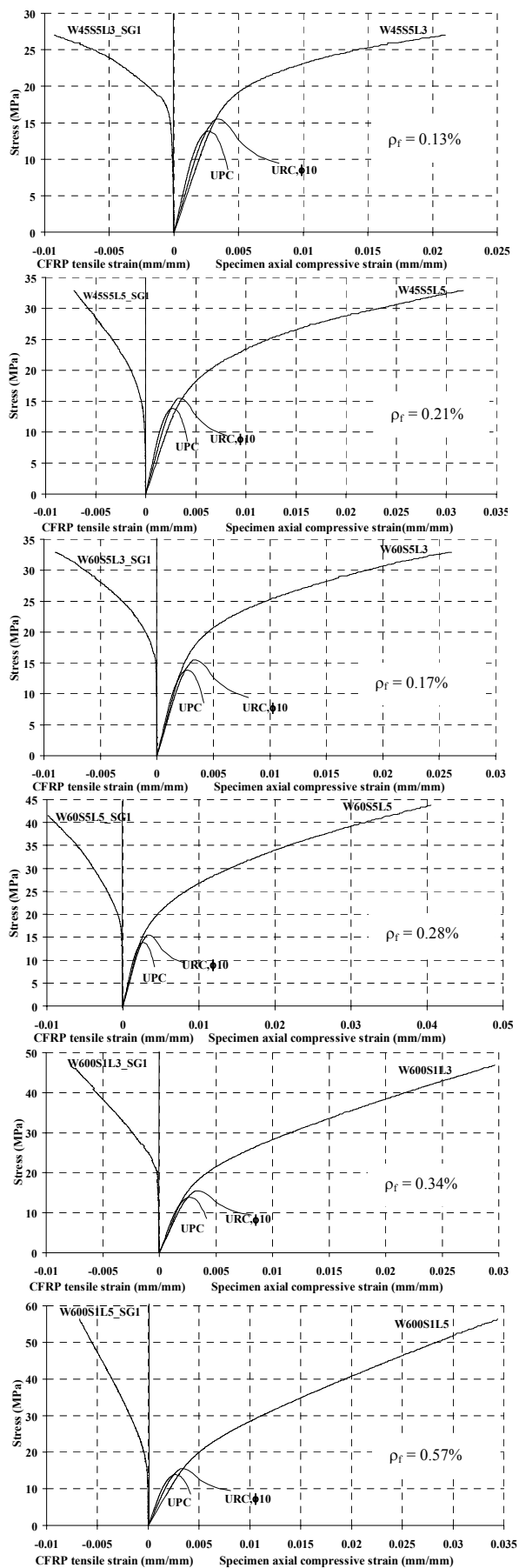


Fig. 5. Test group C15S200φ10.

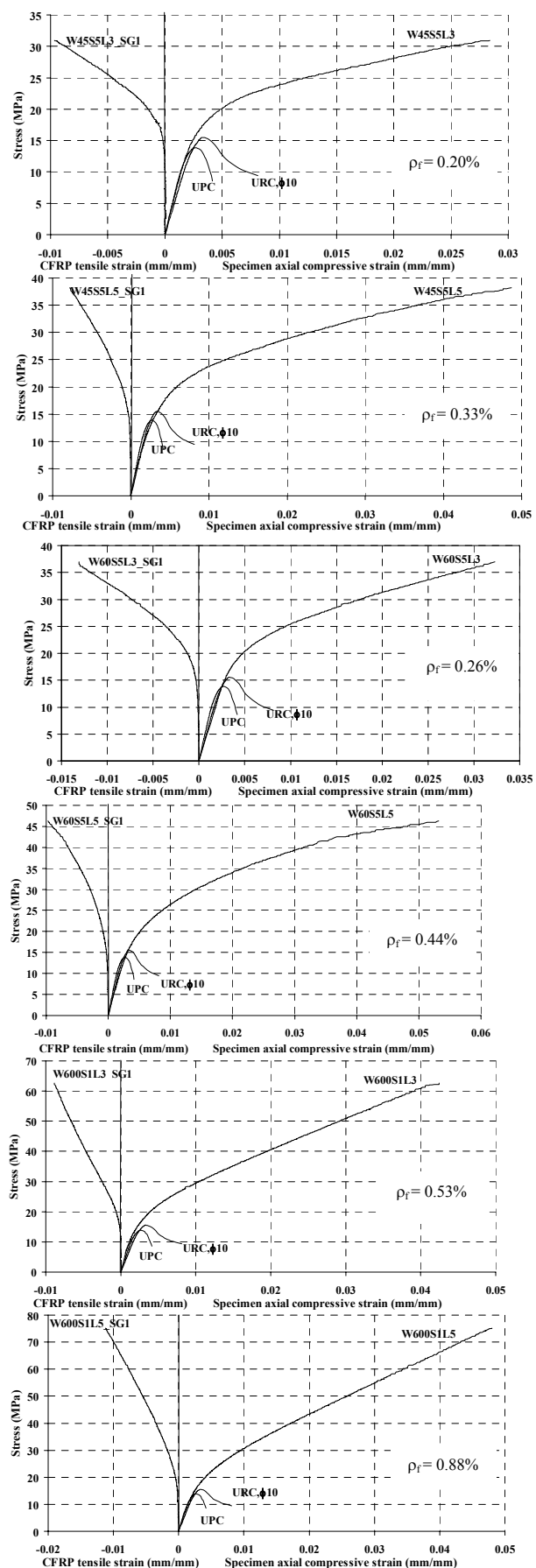


Fig. 6. Test group C15S300φ10.

Tabs. 3 and 4 include the main indicators of the efficacy provided by the applied confinement systems. In these tables,  $f_{co,UPC}$  is the compressive strength of unconfined plain concrete specimens (UPC),  $f_{co,\phi10}$  is the compressive strength of unconfined reinforced concrete specimens (URC, $\phi10$ ),  $\varepsilon_{co,UPC}$  is the specimen axial strain corresponding to  $f_{co,UPC}$ ,  $\varepsilon_{co,\phi10}$  is the specimen axial strain corresponding to  $f_{co,\phi10}$ ,  $f_{cc}$  is the compressive strength (corresponding to the specimen's failure) of confined specimens,  $\varepsilon_{cc}$  is the specimen axial strain corresponding to  $f_{cc}$ ,  $\varepsilon_{fmax}$  is the maximum tensile strain in the CFRP fiber's direction and  $\varepsilon_{fu}$  is the CFRP ultimate strain indicated in Tab. 2. Each value of Tabs. 3 and 4 is the average of the values obtained in the two specimens of each series.

**Tab. 3.** Main indicators of the efficacy of the confinement systems in the C15S200 $\phi10$  test group.

Specimen designation	S	L	$\rho_f$ [%]	$f_{cc}$ (MPa)	$\varepsilon_{cc}$ ( $\mu m/m$ )	$f_{cc}/f_{co,\phi10}$	$\varepsilon_{cc}/\varepsilon_{co,\phi10}$	$\varepsilon_{fmax}$ ( $\mu m/m$ )	$\varepsilon_{fmax}/\varepsilon_{fu}$
Uncon. Plain Conc. (UPC)				13.87 ( $f_{co,UPC}$ )	0.0027 ( $\varepsilon_{co,UPC}$ )	-	-	-	-
Uncon. $\phi10$ Reinf. Conc.				15.52 ( $f_{co,\phi10}$ )	0.0033 ( $\varepsilon_{co,\phi10}$ )	-	-	-	-
W45S5L3	5	3	0.13	27.04	0.021	1.74	6.36	0.00924	0.596
W45S5L5		5	0.21	32.89	0.032	2.12	9.70	0.00717	0.463
W60S5L3	5	3	0.17	32.92	0.026	2.12	7.88	0.00901	0.581
W60S5L5		5	0.28	43.81	0.040	2.82	12.12	0.00989	0.638
W600S1L3	1	3	0.34	46.88	0.030	3.02	9.09	0.00783	0.505
W600S1L5		5	0.57	56.38	0.034	3.63	10.30	0.00675	0.435

**Tab. 4.** Main indicators of the efficacy of the confinement systems in the C15S300 $\phi10$  test group.

Specimen designation	S	L	$\rho_f$ [%]	$f_{cc}$ (MPa)	$\varepsilon_{cc}$ ( $\mu m/m$ )	$f_{cc}/f_{co,\phi10}$	$\varepsilon_{cc}/\varepsilon_{co,\phi10}$	$\varepsilon_{fmax}$ ( $\mu m/m$ )	$\varepsilon_{fmax}/\varepsilon_{fu}$
Uncon. Plain Conc. (UPC)				13.87 ( $f_{co,UPC}$ )	0.0027 ( $\varepsilon_{co,UPC}$ )	-	-	-	-
Uncon. $\phi10$ Reinf. Conc.				15.52 ( $f_{co,\phi10}$ )	0.0033 ( $\varepsilon_{co,\phi10}$ )	-	-	-	-
W45S5L3	5	3	0.20	30.96	0.028	1.99	8.48	0.00965	0.623
W45S5L5		5	0.33	38.23	0.049	2.46	14.85	0.00784	0.506
W60S5L3	5	3	0.26	36.95	0.032	2.38	9.70	0.01310	0.845
W60S5L5		5	0.44	46.29	0.053	2.98	16.06	0.00967	0.624
W600S1L3	1	3	0.53	62.70	0.045	4.04	13.64	0.00887	0.572
W600S1L5		5	0.88	75.12	0.048	4.84	14.55	0.0112	0.72

From the analysis of Figs. 7 and 8 and the results included in Tabs. 3 and 4 it can be concluded that  $f_{cc}/f_{co,\phi10}$  increased with  $\rho_f$ . Fig. 7 shows that this increase is almost linear in the considered  $\rho_f$  range.  $f_{cc}/f_{co,\phi10}$  has varied from 1.7 in series confined with strips CF 120 of 45 mm width and three layers per width (W45S5L3),  $\rho_f=0.13\%$ , up to 4.8 in series fully-wrapped with five layers of CF-130,  $\rho_f=0.88\%$ .

The specimen ultimate axial strain,  $\varepsilon_{cc}$ , has also increased significantly with  $\rho_f$ . The limits of  $\varepsilon_{cc}/\varepsilon_{co,\phi10}$  varied from 6.4 to 16.1. In Figure 8 the  $\varepsilon_{cc}/\varepsilon_{co,\phi10}$  of the fully-wrapped series were not included since their consideration will lose the linear increase trend between  $\varepsilon_{cc}/\varepsilon_{co,\phi10}$  and  $\rho_f$ . The increase of  $\varepsilon_{cc}/\varepsilon_{co,\phi10}$  with  $\rho_f$  was more pronounced in specimens of discrete confinement arrangements than in fully-wrapped specimens. The plastic deformation of the concrete in-between the CFRP strips can justify this occurrence.

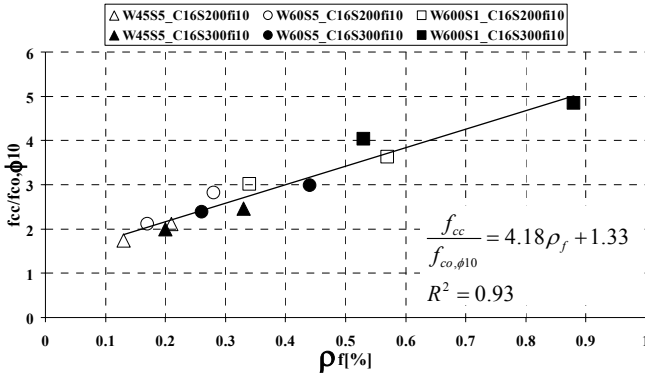


Fig. 7.  $f_{cc}/f_{co,\phi10}$  vs.  $\rho_f$  for C15S200 $\phi$ 10 and C15S300 $\phi$ 10 groups.

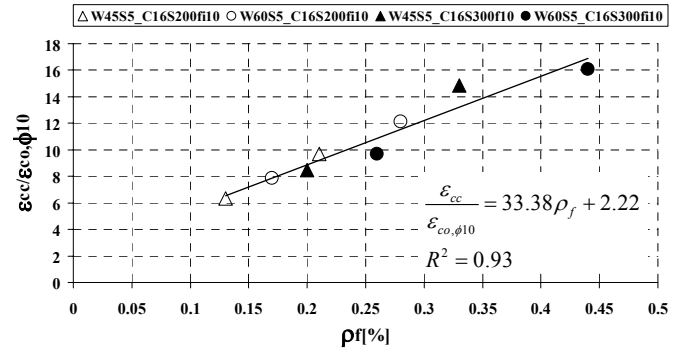


Fig. 8.  $\varepsilon_{cc}/\varepsilon_{co,\phi10}$  vs.  $\rho_f$  for C15S200 $\phi$ 10 and C15S300 $\phi$ 10 groups.

### Groups C32S200 $\phi$ 8 and C32S300 $\phi$ 8

Figs. 9 and 10 show the relationships between concrete stress and both the concrete axial strain and the CFRP strain in the fiber direction for the groups of tests C32S200 $\phi$ 8 and C32S300 $\phi$ 8.

Like in the C15S200 $\phi$ 10 and C15S300 $\phi$ 10 groups of tests, in general, the concrete stress-strain relationship of the confined specimens of groups C32S200 $\phi$ 8 and C32S300 $\phi$ 8 is composed by two quasi-linear branches, connected by a nonlinear transition branch. Tabs. 5 and 6 include the main indicators of the efficacy provided by the applied confinement arrangements.

The load carrying capacity of the test equipment was attained in the W600S1L5 series of C32S200 $\phi$ 8 group and in the W60S6L5, W600S1L3 and W600S1L5 series of C32S300 $\phi$ 8 group, without the occurrence of the rupture of the specimens. Since the load carrying capacity of the equipment can be doubled if the tests are carried out in a non-closed loop control, the specimens of these series were again tested, up to its failure, and the attained  $f_{cc}$  values are indicated in Tabs. 5 and 6 into square brackets. The relationship between  $f_{cc}/f_{co,\phi8}$  and  $\rho_f$ , represented in Fig. 11, shows a linear increasing trend between these two parameters. In this figure, the  $f_{cc}$  corresponds to the compressive strength at the failure of the specimens. Fig. 12 shows that  $\varepsilon_{cc}/\varepsilon_{co,\phi8}$  has also a linear increase trend with the increase of  $\rho_f$ . Since in the manually controlled tests the strains were not measured, this figure only includes the results obtained in the specimens that failed when the tests were carried out under closed loop control.



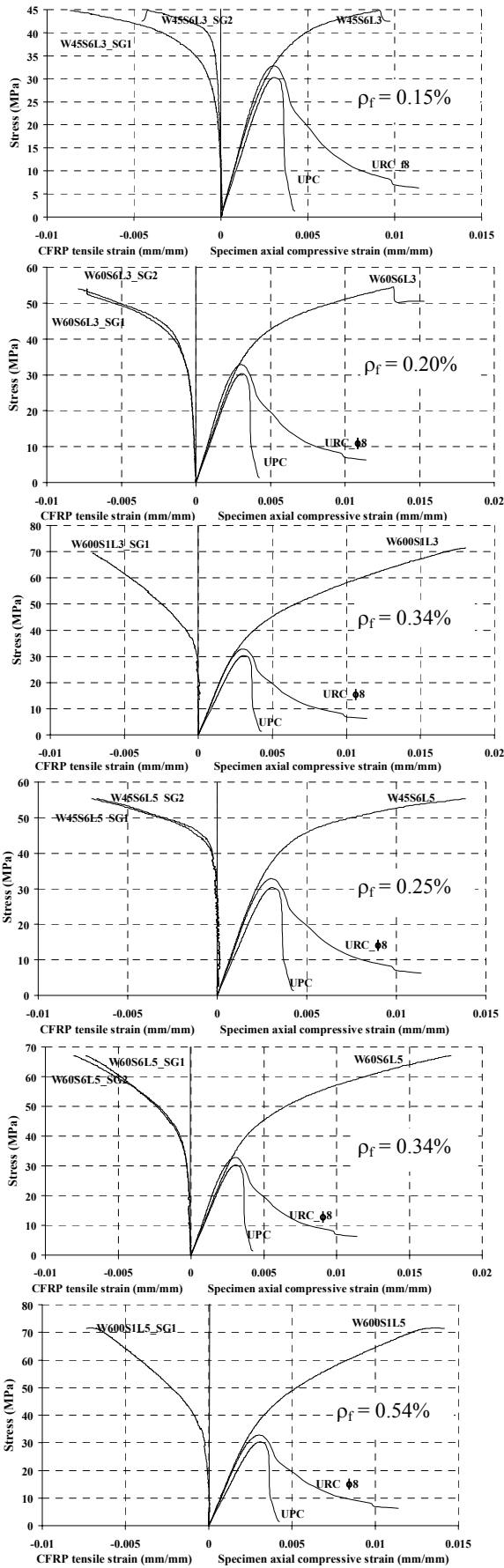


Fig. 9. Test group C32S200φ8.

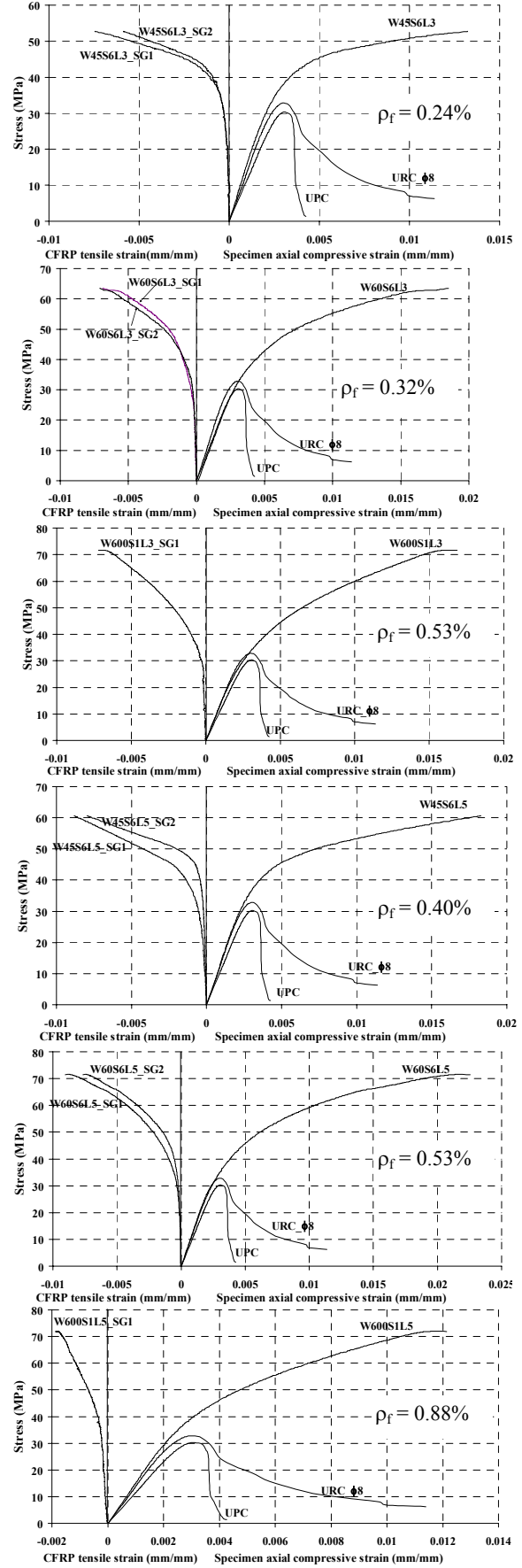


Fig. 10. Test group C32S300φ8.



**Tab. 5.** Main indicators of the efficacy of the confinement systems in the C32S200 $\phi$ 8 test group.

Specimen designation	S	L	$\rho_f$ [%]	$f_{cc}$ (MPa)	$\varepsilon_{cc}$ ( $\mu\text{m}/\text{m}$ )	$f_{cc}/f_{co,\phi 8}$	$\varepsilon_{cc}/\varepsilon_{co}$	$\varepsilon_{fmax}$ ( $\mu\text{m}/\text{m}$ )	$\varepsilon_{fmax}/\varepsilon_{fu}$
Uncon. Plain Concrete (UPC)				30.31 ( $f_{co,UPC}$ )	0.0031 ( $\varepsilon_{co,UPC}$ )	-	-	-	-
Uncon. $\phi 8$ Reinf. Concrete				32.80 ( $f_{co,\phi 8}$ )	0.0030 ( $\varepsilon_{co,\phi 8}$ )	-	-	-	-
W45S6L3	6	3	0.15	44.80	0.0092	1.37	3.07	0.00867 (SG1)	0.56 (SG1)
								0.00422 (SG2)	0.27 (SG2)
W45S6L5		5	0.25	55.36	0.0139	1.69	4.63	0.00702 (SG1)	0.45 (SG1)
								0.00672 (SG2)	0.43 (SG2)
W60S6L3	6	3	0.20	54.37	0.0137	1.66	4.57	0.00731 (SG1)	0.47 (SG1)
								0.00822 (SG2)	0.53 (SG2)
W60S6L5		5	0.34	67.09	0.0179	2.05	5.97	0.00721 (SG1)	0.47 (SG1)
								0.00804 (SG2)	0.52 (SG2)
W600S1L3	1	3	0.34	71.37	0.0181	2.17	6.03	0.0131 (SG1)	0.85 (SG1)
W600S1L5		5	0.57	71.51 [98.36]	0.014	2.18 [3.0]	4.67	0.00735 (SG1)	0.47 (SG1)

**Tab. 6.** Main indicators of the efficacy of the confinement systems in the C32S300 $\phi$ 8 test group.

Specimen designation	S	L	$\rho_f$ [%]	$f_{cc}$ (MPa)	$\varepsilon_{cc}$ ( $\mu\text{m}/\text{m}$ )	$f_{cc}/f_{co,\phi 8}$	$\varepsilon_{cc}/\varepsilon_{co}$	$\varepsilon_{fmax}$ ( $\mu\text{m}/\text{m}$ )	$\varepsilon_{fmax}/\varepsilon_{fu}$
Uncon. Plain Concrete (UPC)				30.31 ( $f_{co,UPC}$ )	0.0031 ( $\varepsilon_{co,UPC}$ )	-	-	-	-
Uncon. $\phi 8$ Reinf. Concrete				32.80 ( $f_{co,\phi 8}$ )	0.0030 ( $\varepsilon_{co,\phi 8}$ )	-	-	-	-
W45S6L3	6	3	0.24	52.76	0.0132	1.60	4.40	0.00743 (SG1)	0.47 (SG1)
								0.00585 (SG2)	0.38 (SG2)
W45S6L5		5	0.40	60.70	0.0185	1.85	6.17	0.00883 (SG1)	0.57 (SG1)
								0.00796 (SG2)	0.51 (SG2)
W60S6L3	6	3	0.32	63.50	0.0185	1.94	6.17	0.00689 (SG3)	0.44 (SG1)
								0.00711 (SG4)	0.46 (SG2)
W60S6L5		5	0.53	71.52 [77.98]	0.0225	2.18 [2.38]	7.50	0.00902 (SG1)	0.58 (SG1)
								0.00764 (SG2)	0.49 (SG2)
W600S1L3	1	3	0.53	71.56 [93.59]	0.0168	2.18 [2.86]	5.60	0.00718 (SG1)	0.46 (SG1)
W600S1L5		5	0.88	71.88 [116.22]	0.0121	2.19 [3.55]	4.03	0.00188 (SG1)	0.12 (SG1)

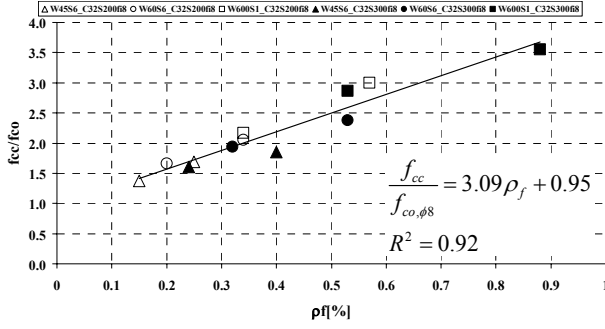


**Fig. 11.**  $f_{cc}/f_{co, \phi 8}$  versus  $\rho_f$  for the specimens of groups C32S200 $\phi$ 8 and C32S300 $\phi$ 8.

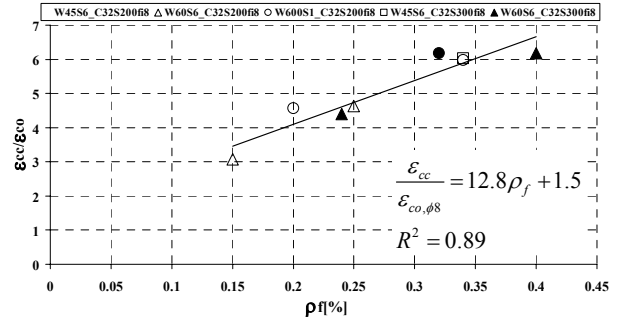


**Fig. 12.**  $\epsilon_{cc}/\epsilon_{co, \phi 8}$  versus  $\rho_f$  for the specimens of groups C32S200 $\phi$ 8 and C32S300 $\phi$ 8.

In series of equal  $\rho_f$ , such is the case of series W60S6L5 and W60S1L3, the confinement was a little bit more effective in the specimens fully wrapped, but the time consumed to fully wrapped the specimens was higher and the failure modes of these specimens were more brittle. The last column of Tabs. 5 and 6 shows that, at the failure of the specimens, which always occurred by the CFRP tensile rupture, the maximum tensile strain in the direction of the fibers,  $\epsilon_{fmax}$ , varied from 27% up to 85% of the CFRP ultimate tensile strain,  $\epsilon_{fu}$ . These values are just for specimens that failed when the equipment was working in closed-loop control. As Lam and Teng have already reported [8], the variation of the strain field in CFRP depends considerably on the distribution of the damage in the concrete specimen. Taking this into account and considering that only one or two strain gauges were applied, per specimen, for recording the CFRP strain variation, it is not surprising that a tendency was not determined for the  $\epsilon_{fmax}/\epsilon_{fu}$  ratio. A high scatter was registered on the maximum strain values in the CFRP, since the recorded values only represent the areas where the strain gauges are placed, and are too dependent on the specimen failure mode configuration. These observations are also applicable to series C15S200 $\phi$ 10 and C15S300 $\phi$ 10, where  $\epsilon_{fmax}$ , varied from 44% up to 84% of the  $\epsilon_{fu}$ .

## NUMERICAL SIMULATION

To simulate the behavior of concrete specimens fully wrapped with CFRP sheets, submitted to direct compressive loading, several analytical models have been proposed [8, 11, 12]. To simulate the behavior of the partially confined concrete specimens tested in the present work, the model developed by Lam and Teng [8] was adopted. According to this model, the stress in the confined concrete ( $\sigma_c$ ) is determined by the following expressions (see Figure 13):

$$\sigma_c = E_c \epsilon_c - \frac{(E_c - E_2)^2}{4f_0} \epsilon_c^2 \text{ for } 0 \leq \epsilon_c \leq \epsilon_t \quad (1)$$

$$\sigma_c = f_0 + E_2 \epsilon_c \text{ for } \epsilon_t \leq \epsilon_c \leq \epsilon_{cc} \quad (2)$$

where  $f_0$  was assumed equal to  $f_{co}$ ,  $\epsilon_t$  is the strain at the transition between the domain of these two equations,

$$\epsilon_t = \frac{2f_0}{(E_c - E_2)} \quad (3)$$

with  $E_2$  being the slope of the equation (2):

$$E_2 = \frac{f_{cc} - f_0}{\epsilon_{cc}} \quad (4)$$

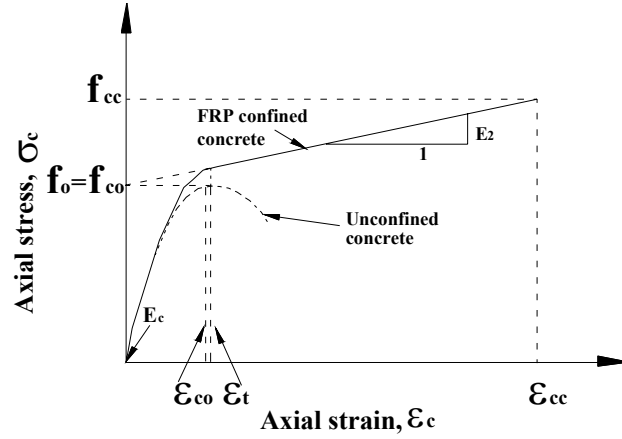


Fig. 13. Stress-strain diagram of Lam and Teng model for FRP confined concrete.

Due to lack of space, only the simulation of one series of the C32S200 $\phi$ 8 and C32S300 $\phi$ 8 groups are represented. Taking the  $f_{cc}/f_{co, \phi 8} - \rho_f$  and  $\epsilon_{cc}/\epsilon_{co, \phi 8} - \rho_f$  relationships included into Figs. 11 and 12 and adopting for  $E_c$  the value (14166 MPa) obtained from the stress-strain curves of the URC\_ $\phi$ 8 specimens, the analytical and experimental stress-strain axial relationships ( $\sigma_c - \epsilon_c$ ) are compared in Figure 14. For the remaining series the degree of accuracy of the simulation was similar to the one obtained for the simulated cases.

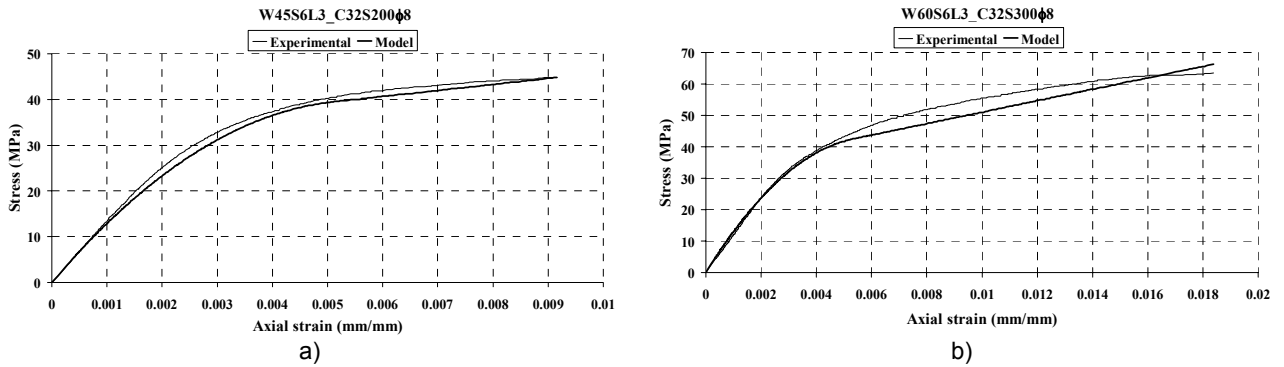


Fig. 14. Comparison between analytical model and experimental results for the: a) W45S6L3 of C32S200 $\phi$ 8 and b) W60S6L3 of C32S300 $\phi$ 8.

## CONCLUSIONS

The present work dealt with an experimental research involving the use of carbon fiber reinforced polymer (CFRP) wet lay-up sheets to increase the load carrying capacity and the deformation ability of reinforced concrete (RC) elements submitted to direct compressive loading. The experimental program was conceived to evidence the influence of fully and partially wrapped confinement arrangements in the compression behavior of this type of elements. Series of tests of two concrete strength classes ( $f_{cm}$  of 15 and 32 MPa), two longitudinal steel reinforcement ratios ( $\rho_{sl}$  of 0.64% and 1%), two transversal steel reinforcement ratios ( $\rho_{st}$  of 0.24% and 0.29%), and two thicknesses for the CFRP sheets ( $t_f$  of 0.113 mm and 0.176 mm) were carried out to assess the influence of these parameters on the confinement performance provided by the confinement arrangements analyzed. In the partial wrapping systems, the distance and width of the CFRP strips were also parameters considered in the experimental program.

From the results obtained in the C15S200 $\phi$ 10 and C15S300 $\phi$ 10 group of tests (average compressive strength of 15 MPa and confined by CFRP sheets of 0.113 mm and 0.176 mm thickness, respectively) the following main observations can be pointed out:

- The compressive strength ratio,  $f_{cc}/f_{co, \phi 10}$  increased from 1.7 for  $\rho_f=0.13\%$  up to 4.8 for  $\rho_f=0.88\%$ ;
- The  $\epsilon_{cc}/\epsilon_{co, \phi 10}$  varied from 6.4 for  $\rho_f=0.13\%$  up to 16.1 for  $\rho_f=0.44\%$ ;
- The maximum strains in the CFRP fiber direction varied from 44% to 84% of the CFRP ultimate strain.

From the results obtained in the C32S200 $\phi$ 8 and C32S300 $\phi$ 8 (average compressive strength of 32 MPa and confined by CFRP sheets of 0.113 mm and 0.176 mm thickness, respectively) the following main observations can be pointed out:

- The compressive strength ratio,  $f_{cc}/f_{cc,08}$  increased from 1.37 for  $\rho_f=0.15\%$  up to 3.55 for  $\rho_f=0.88\%$ ;
- The  $\varepsilon_{cc}/\varepsilon_{co}$  ranged from 3.0 for  $\rho_f=0.15\%$  up to 7.5 for  $\rho_f=0.53\%$ ;
- For the specimens that, when failed, the strains in the fiber direction of the CFRP were registered, the maximum strain varied from 27% up to 58% of the CFRP ultimate tensile strain;

For all test groups it was verified that:

- A linear increasing trend was observed between  $f_{cc}/f_{co}$  and  $\rho_f$ ;
- For the partial-wrapping arrangements, the  $\varepsilon_{cc}/\varepsilon_{co}$  ratio increased almost linearly with  $\rho_f$ ;
- The increase of  $\varepsilon_{cc}/\varepsilon_{co}$  with  $\rho_f$  was not so pronounced in fully-wrapped specimens than in partially confined specimens, since in these last ones a high concentration of concrete plastic strain occurred in the concrete between CFRP strips.

In general, for the specimens of equal  $\rho_f$ , the load carrying capacity of partially confined specimens was a little bit lower than the one of the fully confined specimens. Partial confinement arrangements were, however, easier and faster to apply than full confinement arrangements.

The Lam and Teng model predicted, with enough accuracy, the specimen compressive stress-strain relationship registered in the experiments.

## ACKNOWLEDGMENTS

The authors wish to acknowledge the support provide by *degussa* Portugal and S&P Clever Reinforcement. The first author would like to thank the financial support provided by PRODEP action 5.3/N/199.014/01.

## REFERENCES

1. Seible F, Priestley MJN, Hegemier GA, Innamorato D. Seismic retrofit of RC columns with continuous carbon fiber jackets. *Journal of Composites for Construction*, 1997;1(2): 52-62.
2. Xiao Y, M GR. Seismic retrofit of RC circular columns using prefabricated composites jacketing. *Journal of Structural Engineering*, 1997; 123(10): 1357-1364.
3. Xiao Y, Wu H, Martin, GR. Prefabricated composite jacketing of RC columns for enhanced shear strength. *Journal of structural Engineering*, 1999;124(3): 255-264.
4. Saafi M., Toutanji HÁ, Li Z. Behavior of concrete columns confined with fiber reinforced polymer tubes. *ACI Material Journal*, 1999;96(4):500-509.
5. Cole C, Belardi A. FRP jacketed Reinforced Concrete Columns. *Technical report*, Center for infrastructure engineering studies, Univ. of Missouri, Dep. of Civil Engineering, Rolla, May 2001; USA.
6. ACI Committee 440. Guide for the design and construction of externally bonded FRP systems for strengthening concrete structures. *American Concrete Institute*, 2002.
7. Barros JAO, Ferreira DRSM. Partial versus full wrapping confinement systems for concrete columns. To be published in the *International Conference on Concrete Repair, Rehabilitation and Retrofitting*, South Africa, November 2005.
8. Lam L, Teng JG. Design-oriented stress strain model for FRP-confined concrete. *Construction and building materials Journal*, 2003;17: 471-489.
9. Ferreira DRSM, Barros JAO. *Partial and full confinement of concrete elements using CFRP sheets. Technical report 04-DEC/E-29*, Dep. of Civil Eng., School of Eng., University of Minho, 2004. (in Portuguese)
10. ISO TC 71/SC 6 N. Non-conventional reinforcement of concrete-test methods-part 2: Fiber reinforced polymer (FRP) sheets. *International standard*, 2003.
11. Samaan M, Mirmiran A, Shahawy M. Model of concrete confined by fiber composites. *Journal of Structural Engineering, ASCE*, 1998;124(9): 1025-1031.
12. Toutanji HA. Stress-strain characteristics of concrete columns externally confined with advanced fiber composites sheets. *ACI Material Journal*, 1999;96(3): 397-404.